

New Evidences of Accelerating Degradation of Polyethylene by Starch

Xingxun Liu,^{1,2} Long Yu,^{1,2} Fengwei Xie,³ Eustathios Petinakis,² Parveen Sangwan,² Shirley Shen,² Katherine Dean,² Anne Ammala,² Susan Wong-Holmes²

¹Centre for Polymers from Renewable Resources, SCUT, Guangzhou, 510640, China

²CSIRO, Materials Science and Engineering, Clayton South, Victoria, 3169, Australia

³Australian Institute for Bioengineering and Nanotechnology, UQ, Queensland, Australia

Correspondence to: X. Liu (E-mail: msxxliu@scut.edu.cn) or L. Yu (E-mail: long.yu@csiro.au)

ABSTRACT: An investigation into the effects of starch on both, UV photo-oxidative degradation and biodegradation, of HDPE was focused on the interface between HDPE and starch using Synchrotron-FTIR microscope (SFTIR-M) and scanning electronic microscope (SEM). Carbonyl group detection by FTIR was conducted to evaluate the effect of degradation following exposure to UV photo-oxidative degradation. The results showed that the concentration of carbonyl groups on the interface were higher, suggesting the role of starch in accelerating the UV photo-oxidative degradation of HDPE. The interface between HDPE and starch was further observed under SEM to study the morphological changes after UV photo-oxidative degradation and biodegradation. Micro-cracking was observed on the interface between starch and HDPE after UV photo-oxidative degradation. Tensile testing after UV exposure showed that the variation rate of elongation was higher for the samples containing starch. Starch, an easily biodegradable material, can also act as initial source of nutrients for micro-organisms (bacteria, fungi, and algae) in the blend materials thus enhancing their biodegradability. © 2013 Wiley Periodicals, Inc. *J. Appl. Polym. Sci.* 000: 000–000, 2013

KEYWORDS: biodegradable; blends; degradation; polyolefins; surfaces and interfaces

Received 8 February 2013; accepted 17 April 2013; Published online

DOI: 10.1002/app.39421

INTRODUCTION

Development of degradable polyolefin has attracted increasing interest due to their low price, useful properties, broad suppliers, and mature processing facilities and techniques. UV-oxidative degradation and blending with natural polymers can enhance their biodegradability.^{1–6} Oxo-degradation incorporates oxygen into the carbon chain and results in the formation of functional groups such as carboxylic or hydro-carboxylic acids, esters, aldehydes, and alcohols. This process can be accelerated by exposure of samples to ultraviolet (UV) light or heating. It is suggested that once the molecular weight of a polymer is significantly reduced during oxo-degradation, the oxidized products are deemed susceptible to further degradation by various micro-organisms, which assimilate the oxidized fragments and convert them into CO₂, H₂O, and biomass.^{7,8}

Photo-oxidative degradation is the process of degradation of the material by the action of light and the free radical chain degradation.^{9–11} Rate of abiotic oxidation of polyolefins is important as it determines the rate of subsequent biodegradation process. It has been reported that to achieve significant biodegradation in a reasonable time period, the average molecular weight of oxidized polyolefin should be less than 5000 Da.^{7,8,12–19}

Transition metal salts and transition metal free systems have been widely used as prodegradants to accelerate the oxidation process of polyolefins, as the metal ions can absorb some of radiant energy and transform it to the polymer chain to accelerate its fragmentation. Various Fe and Co-based pre-degradants are commercial available in the market.⁴ Recently, it was found that hydrophilic polymers such as starch^{20–22} and cellulose²³ play an important role in accelerating the degradation of polyolefin in a photo-degrading environment. It has been reported that addition of starch influence the molecule weight of low-density polyethylene (LDPE), resulting into significant reduction in the molecular weight of starch/LDPE blends on exposure to UV radiations.²¹ Raquez et al.²² studied degradability of LDPE using thermal analysis and scanning electron microscope (SEM) and found that oxidative degradations of oxo-degradable LDPE was enhanced with thermoplastic pea starch (TPPS) under UV-condition.

Previous studies^{1,24–26} have also shown that starch can accelerate the oxidative degradation of polyolefin blends and encourage their biodegradation by micro-organisms (bacteria, fungi, and algae)^{1,24–27}. However, there is no clear understanding of the mechanism by which starch influences degradation process of

polyolefin–starch blends. To further explore the degradation mechanisms, it is important to study both chemical and physical changes in the interface between starch and polyolefin, and identify the stage at which acceleration starts.

Theoretically, one can concentrate a Fourier transform infrared (FTIR) beam in a smaller region but that will result in lower sensitivity for a normal FTIR instrument. In comparison, Synchrotron FTIR has a much higher signal-to-noise (S/N) ratio and higher spatial resolution, which allows mapping of the microstructure, as well as providing insight into the chemical distribution and interactions.²⁸ FTIR-microspectroscopy (FTIRM) is the combination of light microscope and infrared spectroscopy. The light microscope is used to magnify structural detail in the sample, whereas infrared spectroscopy provides information on the chemical composition of the sample at specific point. The attenuated total reflection (ATR) accessory is the optical technique used for infrared analysis of polymer surface.^{29,30} The synchrotron-FTIRM can improve the spatial resolution due to its higher brilliance than a routine source.^{31,32} The technology of synchrotron-FTIRM with ATR accessory promises to be a powerful tool in investigating the interface between polymers.

In this study, the investigation of the effects of starch on both UV photo-oxidative degradation and biodegradation of HDPE was focused on the interface between HDPE and starch using Synchrotron-FTIRM and SEM. In addition, variation rates of tensile properties after UV exposure were also investigated.

EXPERIMENTAL

Materials and Sample Preparation

Commercially available HDPE (Etilinas HD5301) with MFI of 9 g/10 min (21.6 kg load) from Petronas, Malaysia was used in this study. Commercially available cornstarch with average particular size (diameter) 36 μm was supplied by Penford (Australia). The starch was dried under vacuum condition at 120°C for 4 h and the final moisture level was less than 0.8%. The blending materials (HDPE 80/starch 20) were compounded using a Theysohn twin-screw extruder ($\varnothing = 30$ mm, L/D = 40) with the highest temperature of 200°C. Fe-base pro-degradant (0.32%) was added into HDPE during extrusion. Pure HDPE was also extruded under the same conditions to be used as a reference. The compounded materials were used to produce film with about 0.2 mm thickness using a Haake single extruder ($\varnothing = 19$ mm, L/D = 19) with a sheet die (150 mm wide) at temperature 190°C.

UV Degradation and Biodegradation

Film samples were exposed to accelerated UV exposure using a QUV-A weatherometer (Q-Panel, 340 nm lamps), with a 20 h UV/4 h condensation exposure in cycle in accordance with ASTM D5208. The film samples were collected and evaluated after different UV exposure times.

For biodegradation experiments, mature compost samples (aged approximately 2–3 months) were collected from a commercial composting facility (NRS Victoria, Australia). Test specimens were cut into film samples (10 mm \times 20 mm) and mixed with the compost (pH 8.4, moisture 48%) in a 3 L glass vessel

according to a standard procedure outlined in AS ISO 14855. A continuous air-flow and temperature range between 55–58°C was maintained throughout the test. The specimens of HDPE/starch blend were collected for analysis after 20 days of aerobic composting, while specimen of neat HDPE was collected for analysis after incubation for 200 days.

Fourier Transform Infrared Spectroscopy (FTIR)

A FTIR with attenuated total reflectance (ATR) was used to detect the carbonyl group on the surface of the specimen. A Nicolet Nexus-670 FTIR equipped with a DTGS detector was employed in this study. A smart orbit diamond ATR sampling accessory was employed for FTIR-ATR experiments. Each spectrum represents 128 co-added scans measured at a spectral resolution of 4 cm^{-1} in the 4000–800 cm^{-1} range. Spectral data were acquired and analyzed with Omnic software version 8.0.

Synchrotron-FTIRM

Synchrotron FTIR microscope was used to study the vertical cross-section of the films. The specimen used for studying interface was cut from the extruded film. The film was embedded into epoxy resin so that vertical cross-section was exposed. The resin was cured overnight at room temperature and then broken in liquid nitrogen. The samples were analysed using a Bruker Vertex V80v Fourier transform infrared (FTIR) spectrometer coupled with a Hyperion 2000 microscope equipped with a liquid nitrogen cooled narrow-band MCT detector at the Australian Synchrotron infrared beamline. A diamond attenuated total reflectance (ATR) was used to collect FTIR spectra. Starch particles were found out by polarizer light first and then analyzed in ATR mode using a 5 $\mu\text{m} \times 5 \mu\text{m}$ aperture with 64 co-added sample scans per position and 64 co-added background scans using OPUS 7.0 software.

Morphological Studies

A Phillips XL-30 FEGSEM SEM (scanning electronic microscope) was used to investigate the morphological variation of the film after UV degradation and biodegradation, in particular the surface of the film samples. Epoxy bars containing sample were immersed in liquid nitrogen and then broken to produce fracture surface specimens. The specimens were coated with

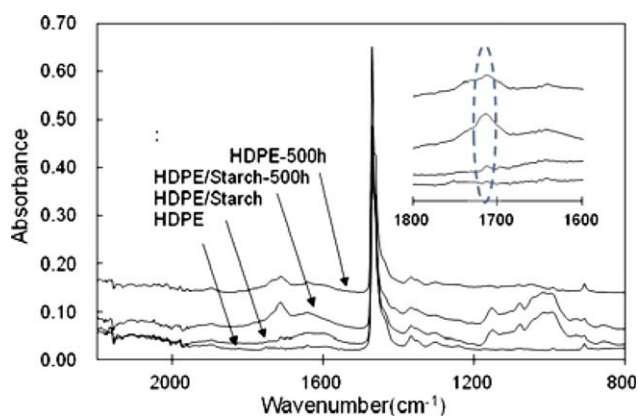


Figure 1. FTIR spectra of virgin pure HDPE and HDPE/starch blend before and after UV exposure for 500 h. [Color figure can be viewed in the online issue, which is available at wileyonlinelibrary.com.]

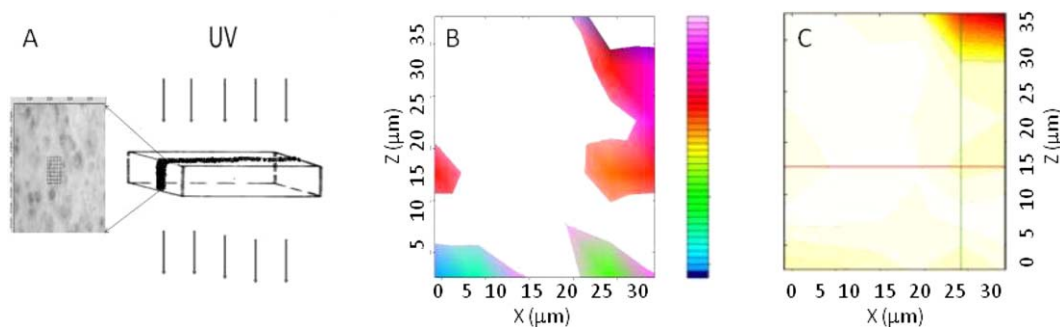


Figure 2. Area measured by Synchrotron-FTIR and the FTIR maps based on carbonyl group. [Color figure can be viewed in the online issue, which is available at wileyonlinelibrary.com.]

iridium in a vacuum evaporator and viewed in the SEM at a low accelerating voltage of 2 kV.

Tensile Testing

Tensile properties of dumb-bell shaped specimens were measured in accordance with ASTM D638 using an Instron mechanical testing apparatus (model 3366). Tensile strength and elongation were measured at a crosshead speed of 5 mm/min.

RESULTS AND DISCUSSION

Figure 1 shows the FTIR-ATR spectra of pure HDPE and HDPE/starch before exposure and after 500 h of UV exposure respectively. The differences among these samples could be clearly observed. The peaks from 1300 to 800 cm^{-1} are for starch, which is due to the C–C, C–O, C–H stretching, and COH bending vibration, as being reported in many previous articles.^{24,33} In the FTIR-ATR spectra of pure HDPE and HDPE/starch blends after UV degradation, there was a new peak at $ca.1800$ – 1680 . A few other familiar peaks were also observed and these were assigned to the carbonyl bands (C=O) stretching vibrations in aldehydes and/or esters (1733 cm^{-1}) carboxylic acid groups (1700 cm^{-1}) and γ -lactones (1780 cm^{-1}).² The carbonyl index (absorbance peak area of the carbonyl group rationed to that of a references absorption peak area at C–C) has been widely used to quantitatively evaluate the UV degradation of HDPE.^{2,35,36} In this study, it was observed that the carbonyl group absorption peak of HDPE/starch blends was higher than that of HDPE after UV treatment for 500 h. The carbonyl index (the ratio of integral from 1731 – 1693 cm^{-1} to integral 1500 – 1417 cm^{-1}) of HDPE and HDPE/starch blends were

0.03 and 0.17 , respectively, which indicated that the presence of starch in the blends accelerated the degradation of HDPE on UV exposure. These results are in agreement with previous reports.²² It has been generally accepted that the photo-oxidation could reduce the crystallinity of the PE after additional of starch, which results in decreasing thermal and UV stability.^{9–11}

Although FTIR-ATR can provide a quantitative data to evaluate the degradation of sample, it is hard to investigate the degradation process at a certain position or the stage of initiation of the degradation process. The start point is a very important scientific issue, which can further elucidate the degradation mechanisms involved. In this study, FTIR-microscope with ATR was used to study the chemical composition at micro scale, offering new insight into the distribution of carbonyl index between starch and HDPE. Figure 2(A) shows the schematic representation of the specimen collected from the starch/HDPE film after UV radiation. Figure 2(B) shows the mapped composition of within the selected area of HDPE/starch blends after UV degradation in vertical cross-section. A starch granule in the centre of the film was chosen to study the interface between HDPE and starch. The selected area of HDPE/starch blend imaged by FTIR microscope was observed from the carbonyl index map, and a false colour scheme was established (Figure 2). The white zone in the Figure 2(B) represents starch since it did not contain the carbonyl functional group. The colour in the carbonyl index group map reflected absorbance and level of degradation extent of HDPE in the blend. Red indicates the strongest absorbance and highest level of degradation, whereas blue indicates the

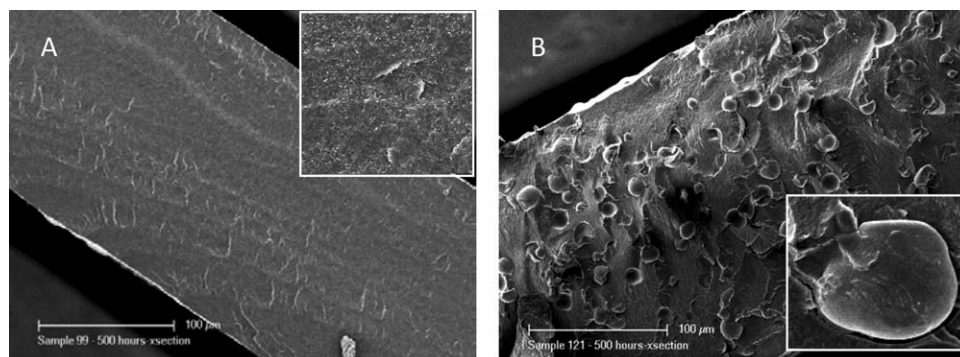


Figure 3. SEM macrographs of the vertical cross-section of pure HDPE (A) and HDPE/starch blend (B) after UV exposure for 500 h.

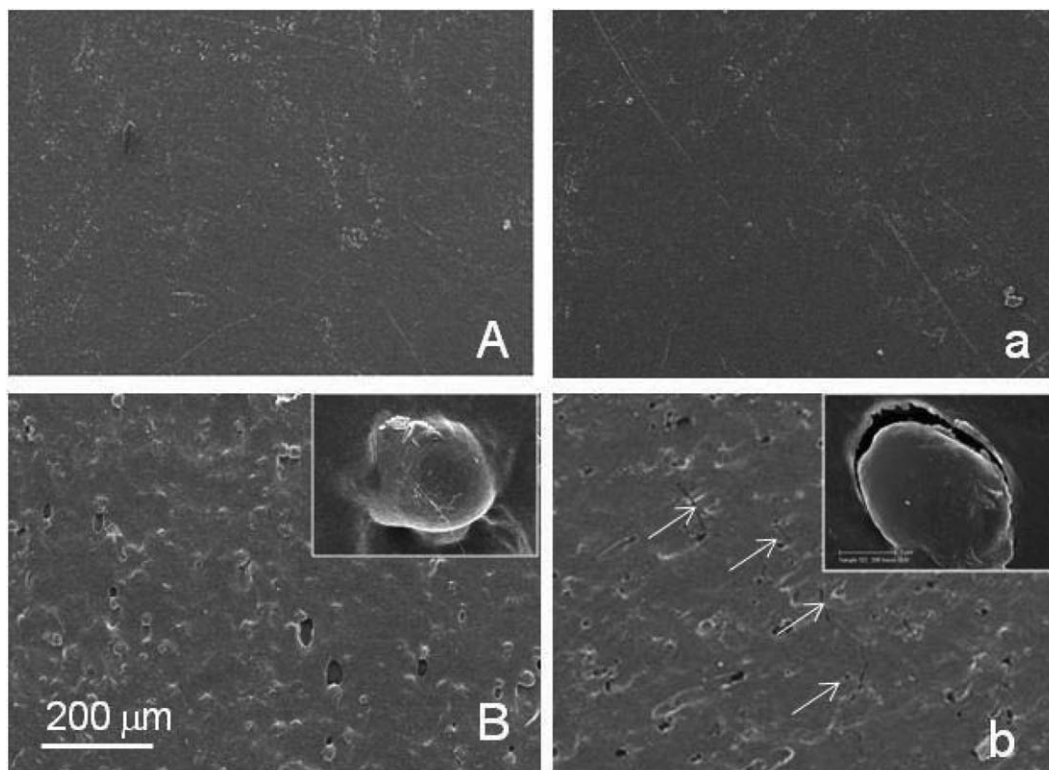


Figure 4. SEM macrographs of the surface of pure HDPE (A,a) and HDPE/starch blend (B,b) before (A,B) and after UV exposure for 500 h (a,b).

lowest value. The carbonyl absorption caused by UV radiation mainly appeared around the starch granule in the specimen, while starch itself treated with UV radiation did not show any changes in FTIR spectra.³⁷ It was interesting to notice from Figure 2(B) that the red color appeared in the interface between starch and HDPE, which indicate degradation started from the interface. These results confirm that starch play an important role in accelerating the degradation of HDPE. Figure 2(C) shows the carbonyl group map (integral from 1731 to 1693 cm^{-1}). Similarly, it was clearly observed that the carbonyl absorption appeared in the interface between starch and HDPE (mainly in HDPE phase). Furthermore, both Figure 2(B) and (C) shows that the oxidation rate expressed by carbonyl index (or carbonyl content) is related to the UV radiation depth, which have been observed by FTIR with variable angle ATR.²

Figure 3 shows the SEM micrographs of the vertical cross-section of pure HDPE and HDPE/starch blend after UV exposure for 500 h. A homogeneous phase for the pure HDPE film was observed after exposing to UV except for a smoother layer in central zone, which might be due to the difference of UV radicalization depth. Gulminea et al.² used varying angle ATR to study the degradation extent of UV radicalization depth and observed that the degradation extent decreased with increasing depth. Some micro-cracks were also noticed and they mainly appeared on the interface between starch and HDPE of the test specimen, HDPE/starch blend.

Figure 4 shows the surfaces of pure HDPE and HDPE/starch blend before and after UV exposure. No differences were

observed for the pure HDPE film even after exposure to UV for 500 h, except for few defects. However, there were many micro-cracks observed on the interface of HDPE/starch blends after UV degradation, which looked similar to as seen in Figure 3. These micro-cracks could cause stress concentration and detrimentally affect the mechanical properties.

The elongation variation rate (%) of samples for pure HDPE and HDPE/starch blend with different UV exposure time are shown in Figure 5. It was observed that the rate (%) increased with an increasing UV exposure time for pure HDPE and

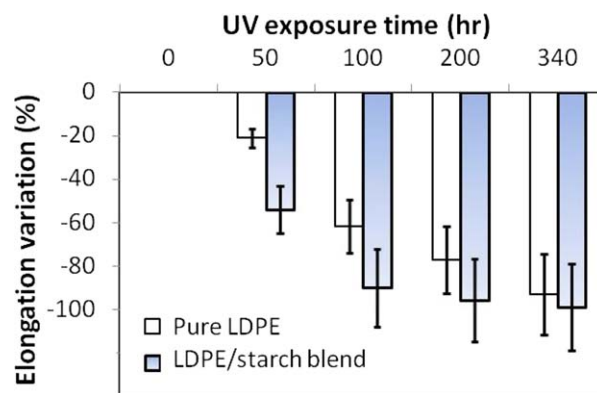


Figure 5. Elongation variable (%) of elongation for pure HDPE (1) and HDPE/starch blend after UV exposure for different time periods. [Color figure can be viewed in the online issue, which is available at wileyonlinelibrary.com.]

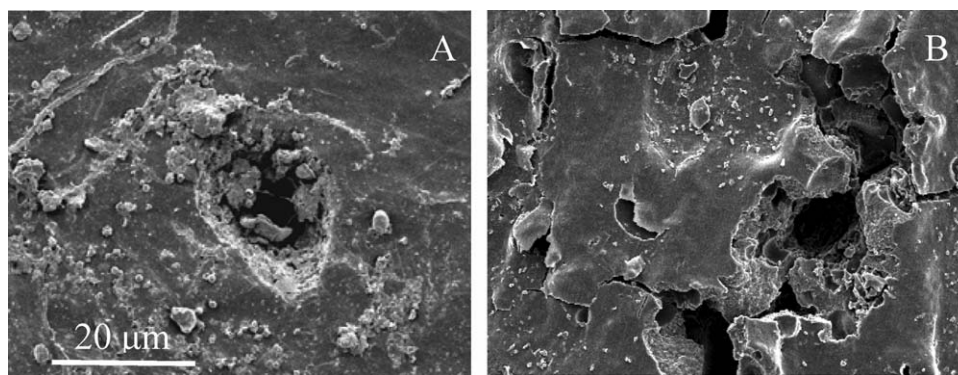


Figure 6. SEM of pure HDPE (A) and HDPE/starch (B) after UV exposure for 500 h then composted in soil for (A) 200 and (B) 20 days, respectively.

HDPE/starch blend; however, the starch increased the decrease rate.

In theory, HDPE consists of only C–C and C–H bonds and does not absorb light in the wavelength region longer than 190 nm, but the impurities which act as initiators could absorb the light at higher wavelength and lead to the generation of free radicals. Usually, this process can be accelerated by metal ions. Starches contain various impurities and hydroxyl functional groups.^{38,39} The UV photo-oxidation degradation is a combined effect of photolysis and oxidative reactions and usually has been as a radical-based oxidative process.^{38–40} The hydroxyl functional groups present in starches could combine with the bronsted acidic to form the catalytic active sites thus accelerating the degradation of HDPE.

Figure 6 shows the SEM images of pure HDPE (A) and HDPE/starch (B) after UV exposure for 500 h and then aerobically composted for 200 (A) and 20 (B) days, respectively. In comparison to pure HDPE film, many holes and cracks were observed in the HDPE/starch film, probably caused due to the microbial attack. The filamentous micro-organisms appended in the films are typical of fungi or actinomycetes. Observably the starch and the macro-cracks (that resulted from UV degradation) acted as initial point of attack by micro-organisms, providing food material and accessibility to the microbial cells to slowly degrade oxidized HDPE/starch blends.

CONCLUSION

To further explore the degradation mechanisms of PE/starch blend, in particular how the starch accelerates the degradation of PE, this study focused on the interface between the two components. The interface between HDPE and starch was investigated by Synchrotron-FTIR microscope and SEM after UV exposure and biodegradation.

The Synchrotron-FTIR shows that concentration of carbonyl groups on the interface was higher. Micro-cracking was observed on the interface between starch and HDPE after UV photo-oxidative degradation by SEM. During the biodegradation of HDPE/starch blends, starch acted as an easily available food-source for micro-organisms (bacteria and fungi) thus supporting their growth and accessibility to bulk material. Tensile

testing showed that the variation rate of elongation was higher after blending with starch. All of these results suggest that starch accelerates both the UV photo-oxidative degradation and biodegradation of PE.

ACKNOWLEDGMENTS

X Liu would like to acknowledge the financial assistance (State Scholarship Fund) provided by China Scholarship Council for his study in Australia. The authors from SCUT, China would like to acknowledge the research funds NSFC (31071503, 21174043), GNSF (S2012040006450), FRFCU (2012ZZ0085, 2012ZB0006) and RFDCU (20110172110027). Australian Synchrotron for radiation source beam time is acknowledged.

REFERENCES

1. Kyrikou, I.; Briassoulis, D. *J. Polym. Environ.* **2007**, *15*, 125.
2. Gulmine, J. V.; Janissek, P. R.; Heise, H. M.; Akcelrud, L. *Polym. Degrad. Stab.* **2003**, *79*, 385.
3. Wiles, D. M.; Scott, G. *Polym. Degrad. Stab.* **2006**, *91*, 1581.
4. Ammala, A.; Bateman, S.; Dean, K.; Petinakis, E.; Sangwan, P.; Wong, S.; Yuan, Q.; Yu, L.; Patrick, C.; Leong, K. H. *Prog. Polym. Sci.* **2011**, *36*, 1015.
5. Elanmugilan, M.; Sreekumar, P. A.; Singha, N. K.; Al-Harathi, M. A.; De, S. K. *J. Appl. Polym. Sci.* **2013**, *129*, 449.
6. Fertier, L.; Koleilat, H.; Stemmelen, M.; Giani, O.; Joly-Duhamel, C.; Lapinte, V.; Robin, J.-J. *Prog. Polym. Sci.* **2013**, *38*, 932.
7. Reddy, M. M.; Deighton, M.; Gupta, R. K.; Bhattacharya, S. N.; Parthasarathy, R. *J. Appl. Polym. Sci.* **2009**, *111*, 1426.
8. Albertsson, A.-C.; Andersson, S. O.; Karlsson, S. *Polym. Degrad. Stab.* **1987**, *18*, 73.
9. Singh, B.; Sharma, N. *Polym. Degrad. Stab.* **2008**, *93*, 561.
10. Scott, G.; Wiles, D. M. *Biomacromolecules* **2001**, *2*, 615.
11. Jeyakumar, D.; Suresh, G.; Mukesh, D. *J. Appl. Polym. Sci.* **2012**, *125*, 2790.
12. Vogt, N. B.; Kleppe, E. A. *Polym. Degrad. Stab.* **2009**, *94*, 659.

13. Chiellini, E.; Corti, A.; Swift, G. *Polym. Degrad. Stab.* **2003**, *81*, 341.
14. Haines, J. R.; Alexander, M. *Appl Microbiol.* **1975**, *29*, 621.
15. Yamada-Onodera, K.; Mukumoto, H.; Katsuyaya, Y.; Saiganji, A.; Tani, Y. *Polym. Degrad. Stab.* **2001**, *72*, 323.
16. Kawai, F.; Watanabe, M.; Shibata, M.; Yokoyama, S.; Sudate, Y.; Hayashi, S. *Polym. Degrad. Stab.* **2004**, *86*, 105
17. Larkin, M. J.; Kulakov, L. A.; Allen, C. C. R. *Curr. Opin. Biotech.* **2005**, *16*, 282.
18. Das, K.; Mukherjee, A. *Appl. Microbiol. Biotechnol.* **2005**, *69*, 192.
19. Breslin, V. T. *J. Polym. Environ.* **1993**, *1*, 127.
20. Morancho, J. M.; Ramis, X.; Fernández, X.; Cadenato, A.; Salla, J. M.; Vallés, A.; Contat, L.; Ribes, A. *Polym. Degrad. Stab.* **2006**, *91*, 44.
21. Erlandsson, B.; Karlsson, S.; Albertsson, A.-C. *Polym. Degrad. Stab.* **1997**, *55*, 237.
22. Raquez, J.-M.; Bourgeois, A.; Jacobs, H.; Degée, P.; Alexandre, M.; Dubois, P. *J. Appl. Polym. Sci.* **2011**, *122*, 489.
23. Kaczmarek, H.; Oldak, D. *Polym. Degrad. Stab.* **2006**, *91*, 2282.
24. Posey, T.; Hester, R. D. *Plast. Eng.* **1994**, *50*, 19.
25. Lee, B.; Pometto, A. L.; Fratzke, A.; Bailey, T. B. *Appl. Environ. Microb.* **1991**, *57*, 678.
26. Albertsson, A.-C.; Barenstedt, C.; Karlsson, S.; Lindberg, T. *Polymer* **1995**, *36*, 3075.
27. Yu, L.; Dean, K.; Li, L. *Prog. Polym. Sci.* **2006**, *31*, 576.
28. Sin, L. T.; Rahman, W. A. W. A.; Rahmat, A. R.; Samad, A. A. *Polymer* **2010**, *51*, 1206.
29. Goormaghtigh, E.; Raussens, V.; Ruyschaert, J.-M. *BBA Biomembranes* **1999**, *1422*, 105.
30. Snabe, T.; Petersen, S. B. *J. Biotechnol.* **2002**, *95*, 145.
31. Wetzel, D. L.; Shi, Y.-C.; Reffner, J. A. *Appl. Spectrosc.* **2010**, *64*, 282.
32. Hirschmugl, C. J.; Bayarri, Z.-E.; Bunta, M.; Holt, J. B.; Giordano, M. *Infrared Phys. Technol.* **2006**, *49*, 57.
33. Capron, I.; Robert, P.; Colonna, P.; Brogly, M.; Planchot, V. *Carbohydr. Polym.* **2007**, *68*, 249.
34. Van Soest, J. J. G.; Tournois, H.; de Wit, D.; Vliegthart, J. F. G. *Carbohydr. Res.* **1995**, *279*, 201.
35. Costa, L.; Luda, M. P.; Trossarelli, L. *Polym. Degrad. Stab.* **1997**, *58*, 41.
36. Dintcheva, N. T.; Al-Malaika, S.; La Mantia, F. P. *Polym. Degrad. Stab.* **2009**, *94*, 1571.
37. Umami-Shafiqah, M. S.; Fazilah, A.; Karim, A. A.; Kaur, B.; Yusup, Y. *Int. Food Res. J.* **2012**, *19*, 265.
38. Grigoriadou, I.; Paraskevopoulos, K. M.; Chrissafis, K.; Pavlidou, E.; Stamkopoulos, T. G.; Bikiaris, D. *Polym. Degrad. Stab.* **2011**, *96*, 151.
39. Yu, L.; Liu, X.; Petinakis, E.; Bateman, S.; Sangwan, P.; Ammala, A.; Dean, K.; Wong-Holmes, S.; Yuan, Q.; Siew, C. K.; Samsudin, F.; Ahamid, Z. *J. Appl. Polym. Sci.* **2013**, *128*, 591.
40. Matuana, L. M.; Jin, S.; Stark, N. M. *Polym. Degrad. Stab.* **2011**, *96*, 97.